THE JOURNAL OF PHYSICAL CHEMISTRY A

Article

pubs.acs.org/JPCA

Salty Glycerol versus Salty Water Surface Organization: Bromide and Iodide Surface Propensities

Zishuai Huang, Wei Hua, Dominique Verreault, and Heather C. Allen*

Department of Chemistry and Biochemistry, The Ohio State University, 100 West 18th Avenue, Columbus, Ohio 43210, United States

ABSTRACT: Salty NaBr and NaI glycerol solution interfaces are examined in the OH stretching region using broadband vibrational sum frequency generation (VSFG) spectroscopy. Raman and infrared (IR) spectroscopy are used to further understand the VSFG spectroscopic signature. The VSFG spectra of salty glycerol solutions reveal that bromide and iodide anions perturb the interfacial glycerol organization in a manner similar as that found in aqueous halide salt solutions, thus confirming the presence of bromide and iodide anions at the glycerol surface. Surface tension measurements are consistent with the surface propensity suggested by the VSFG data and also show that the surface excess increases with increasing salt concentration, similar to that of water. In addition, iodide is shown to have more surface prevalence than bromide, as has also been determined from aqueous solutions. These results suggest that glycerol behaves similarly to water with respect to surface activity and solvation of halide anions at its air/liquid interface.

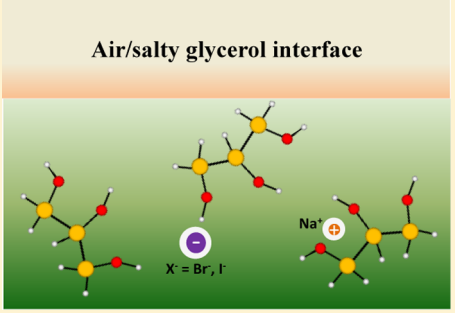

1. INTRODUCTION

Glycerol is a colorless, low toxicity, viscous liquid polyol with three hydroxyl groups, which is moderately hygroscopic and completely miscible with water.[1,2] It also serves as a good protic solvent for many inorganic and organic compounds due to its amphiphilic nature. In part due to its low toxicity, it has a wide range of applications including, among others, its uses as an antifreeze and cryoprotecting agent, as a detergent, and as a moisturizing and lubricating agent in cosmetics and pharmaceutical products.[3] Despite its viscous nature, glycerol shares some physical properties with water such as an extensive hydrogen bonding network, a high surface tension (water, ~72.8 mN/m; glycerol, ~63.4 mN/m at 293 K),[2,4] and a large dielectric constant (water, ~80.2; glycerol, ~41.1 at 293 K).[2,5] Therefore, as a promising proxy for water in research, it is relevant to examine similarities and differences between these two important solvents.

Some work has been done on pure glycerol to explore its bulk and interfacial structures. Champeney et al. studied deuterated glycerol using neutron diffraction in the bulk liquid and proposed that the glycerol structure is highly dependent on hydrogen bonding with neighboring molecules and that all molecules are likely to be interlinked by a sequence of hydrogen bonds.[6] Root and Stillinger using molecular dynamics (MD) simulations obtained a monomer isomer with an extended conformation similar to that found in glycerol crystal.[7] Chelli et al. also studied glycerol condensed phase by MD simulations and focused on the conformational structure and hydrogen bonding.[8] Soltwisch and Steffen concluded from their X-ray scattering experiments that glycerol crystalline conformation is probably predominant in the liquid phase.[9] Different groups using spectroscopic methods such as Raman,[10,11] attenuated total reflection infrared (ATR-IR),[11,12] vibrational sum frequency generation (VSFG) spectroscopy,[13,14] and electron energy loss spectroscopy[15] showed that, both in the bulk and at the interface, pure glycerol exhibits a broad OH stretching band from 3000 to 3600 cm^{-1} characteristic of hydrogen-bonded glycerol molecules. Yet, unlike water, no dangling OH stretch was observed for the pure glycerol surface.[13,14]

With respect to the ion−solvent system, only a few reports about the solvation of ions in glycerol are available.[16,17] Yet, there has been some interest around glycerol surfaces and ion solvation. Nathanson and co-workers used glycerol as a proxy for water in studies of the gas−liquid interactions relevant to atmospheric aerosol chemistry and published much work on interfacial proton exchange between halide acids in the gas phase and glycerol in the presence of alkali halide salts.[18−23]

In contrast, interfacial characteristics of halide aqueous solutions have been extensively studied. For example, Jungwirth and Tobias used MD simulations to study and predict ion surface propensity and solvation at the interface between air and aqueous halide solutions.[24,25] Later, Liu et al., using VSFG as well as IR and Raman spectroscopy, investigated the ion distributions at the surface of aqueous halide solutions and revealed structural differences relative to the neat air/water interface.[26] Baldelli et al.,[27] Raymond et al.,[28] and Tian et al.[29] also used VSFG spectroscopy to probe the hydrogen bonding of aqueous halide solution surfaces. Additionally, Bian et al. also examined the perturbation of various halides on interfacial

Special Issue: Prof. John C. Wright Festschrift

Received: February 26, 2013
Revised: April 24, 2013
Published: May 13, 2013

water organization by using surface second harmonic generation (SHG) spectroscopy.[30]

In this article, we present spectra of sodium halide glycerol solutions in the OH stretching vibrational region using VSFG, Raman, and IR spectroscopy. By comparing the glycerol spectra with spectra of aqueous solutions, differences and similarities associated with glycerol and with water, as well as their interactions with halide anions, are analyzed and discussed. In addition, surface tension measurements on the same solutions have been performed to assess the surface excess of the given solutes. The research presented here was motivated by prior work conducted by Nathanson and co-workers.[19−21] Our findings reveal many similarities between aqueous and glycerol solutions with respect to ion surface propensity of halide salts and solvation.[9−11,21−23]

2. EXPERIMENTAL SECTION

2.1. Materials. Sodium bromide (certified ACS granular, 99.5% purity) and sodium iodide (certified crystalline) were purchased from Fisher Scientific. For purification, all salts were heated at 500 °C for 10 h before dissolving in solvents. Glycerol (≥99% purity) was purchased from Sigma-Aldrich. Nanopure water (not purged of CO_2) with a pH of 5.5 and a resistivity of 18.0 MΩ·cm was obtained from a Barnstead Nanopure system (model D4741, Thermolyne Corporation) equipped with additional organic removing cartridges (D5026 Type I ORGANICfree Cartridge Kit; Pretreat Feed).

2.2. Preparation of Salty Solutions. Halide salt aqueous solutions were prepared by simply dissolving the purified salts in nanopure water. Halide salts were dissolved overnight in the same manner in glycerol assisted with a magnetic hot plate and a stirrer. For convenient comparison with Nathanson's studies,[18,19] 1 and 2 M salt solutions were chosen for both water and glycerol. NaCl was not selected due to its relatively low solubility in glycerol at these concentrations. In addition, all solutions were conditioned at room temperature (23 ± 1 °C) over 24 h prior to any measurement.

2.3. VSFG Spectroscopy. VSFG spectroscopy measurements were performed using a broadband VSFG spectrometer setup that has been described elsewhere.[31−34] Briefly, a titanium:sapphire oscillator (Tsunami, Spectra-Physics) with a center wavelength at 800 nm was used to seed two 1 kHz regenerative amplifiers (Spitfire femtosecond and picosecond versions, Spectra-Physics) that are pumped by a solid-state Nd:YLF laser (Evolution 30, SpectraPhysics) at 527 nm. The amplifiers generate narrowband (2 ps, ∼17 cm^{-1} bandwidth, >0.9 W) and broadband (∼85 fs, ∼345 cm^{-1} bandwidth, ∼1 W) laser pulses at 800 nm.[33] The narrow-bandwidth beam was used as the visible beam, while the broad-bandwidth beam was further directed to an optical parametric amplifier (TOPAS-C, Light Conversion) coupled to a narrow-difference frequency generation system (NDFG, Light Conversion) that generated a tunable mid-IR beam. The full spectral bandwidth of the generated broadband IR beam was ∼800 cm^{-1} in the OH region (3000−3800 cm^{-1}). The average energies of the visible and IR beams for the OH stretching region were 300 and 10 μJ, respectively. Furthermore, the setup was purged with dry nitrogen to minimize the absorption of water vapor in the air in the OH stretching region.

The visible (s-polarized) and IR (p-polarized) beams are spatially and temporally overlapped on the sample's surface (salt solutions and GaAs) at incident angles of ∼59° and ∼63°, respectively, to generate a sum-frequency (SF) beam (s-polarized). The reflected SF beam was then dispersed by a monochromator (SpectraPro SP-500, Acton Research; 1200 g/mm grating blazed at 750 nm) and detected by a liquid-nitrogen-cooled charge-coupled device (CCD) camera (Spec-10:400B, LN400EB back-illuminated, Roper Scientific; 1340 × 400 pixel array). The noise that can contribute to the VSFG spectrum background was subtracted by adjusting the time delay and remeasuring the VSFG background spectrum. (Glycerol is highly viscous, and the surface generates more scattering relative to neat water upon the illumination of the pulsed light and thus contributes to the noise in the spectrum.) Two spectra were averaged for each sample and the acquisition time for each spectrum was set to 5 min. All spectra were obtained at room temperature.

For the studies presented here, it is important to note that the maximum depth that can be probed is determined by the wavelength of the visible beam. However, due to the lack of inversion symmetry and depending on the chemical system, the probe depth can be in the range of 1−3 nm.

2.4. Raman Spectroscopy. The Raman experimental setup consisted of a 532 nm continuous wave laser (Millennia Vs, SpectraPhysics), a Raman probe (RPS532/12-15, InPhotonics), a monochromator (SR-303I-A, Andor Technology; 1200 g/mm grating), and a CCD (Newton EM, DU970N-BV, Andor Technology). Raman spectra were collected in the 0° backscattered direction using a fiber optic, which was coupled to the entrance slit of the monochromator. Andor SOLIS software (version 4.15) was used for data collection and display. The output power of the 532 nm beam exiting the Raman probe was ∼95 mW. Prior to data collection, the Raman system was calibrated with a USB Ne−Ar source (Princeton Instrument) and further fine-calibrated by taking the Raman spectrum of naphthalene powder. Raman spectra were obtained using unpolarized light as the multimode fiber scrambles the polarization from the laser. All samples were prepared in 4 mL pyrex glass vials. All Raman spectra were obtained at room temperature.

2.5. FTIR Spectroscopy. An FTIR spectrometer (Spectrum 100 FTIR Spectrometer, Perkin-Elmer) was employed in the attenuated total reflection Fourier transform infrared (ATR-FTIR) spectroscopy measurements using a 45° incident geometry and a ZnSe crystal mounted to the benchtop of the FTIR spectrometer. Although ATR-FTIR is usually used for interfacial measurements, it was employed here as a bulk interrogation technique due to the fact that the penetration depth using the ATR crystal is on the order of micrometers. In comparison to transmission IR, the ATR mode has also the advantage to avoid signal saturation in the OH stretching region. For each solution, a volume of about 1 mL was deposited on the crystal surface. Spectra were collected using Spectrum Software (version 6.3.4) with a spectral resolution of 4 cm^{-1} and 100 scans at room temperature.

2.6. Surface Tension Measurements. Surface tension was measured using a surface force device from a Langmuir trough system (Minitrough, KSV Instruments). A platinum Wilhelmy plate (measured perimeter of 39.4 mm) was cleaned with concentrated sulfuric acid and flamed using a Bunsen burner before measurements to ensure removal of adsorbed adventitious organic contamination.[35] Measurements were taken by pouring ∼12 mL of salty solutions into a Petri dish and dipping the plate into the liquid surface. Care was taken to place the plate in the center of the dish upon contact with the surface to avoid meniscus effects. The force exerted on the plate

dx.doi.org/10.1021/jp4020228 | J. Phys. Chem. A 2013, 117, 6346−6353

was read in KSV LayerBuilder software (version 2.0.1) and the surface tension was calculated using the Wilhelmy equation.[35]

3. RESULTS AND DISCUSSION

There have been relatively few studies investigating the air/glycerol interface by means of VSFG spectroscopy[13,14] and none so far reporting VSFG spectra of halide salt glycerol solutions. Here, VSFG spectra of NaBr and NaI glycerol solution surfaces are determined in the OH stretching region to understand interfacial organization and solvation for this protic solvent. The OH group is highly sensitive to its environment,[36−42] in particular to solvation of halide anions at the air/glycerol interface and in the bulk phase.[27,28,31,37,43,44] To this end, the VSFG spectra of pure glycerol and water surfaces, essential in understanding interfacial organization of the solvated salt ions, are first shown, followed by bulk measurements using Raman and IR spectroscopy for comparison. Finally, surface tension data on salty glycerol solutions are presented to further discuss halides' surface prevalence.

3.1. Glycerol and Water. The VSFG spectra of the neat air/glycerol and air/water interfaces in the OH stretching region (3000−3800 cm^{-1}) are shown in Figure 1. Both VSFG spectra exhibit broad overlapping resonances extending from 3000 to 3550 cm^{-1} that are assigned to the hydrogen-bonded OH groups of glycerol and water at their respective air/liquid interfaces. The broad band for glycerol is somewhat asymmetric in character with stronger and weaker intensity in the lower (~3100−3300 cm^{-1}) and higher (~3300−3550 cm^{-1}) frequency regions, respectively. Possible contributions from the CH resonant tail cannot be ruled out. The water broad band has more obvious structure and reveals relatively equal intensities for the range from 3150 to 3450 cm^{-1}. Spectral assignments for the neat water VSFG spectrum have been discussed extensively and remain somewhat controversial, especially for the lower frequency region.[42,45−49] It is believed that the broad band ranging from 3000 to ~3600 cm^{-1} reflects the collective OH stretching modes of hydrogen-bonded water molecules that display complex coordination and cooperativity within a few Å below the topmost water surface layer.[29,50]

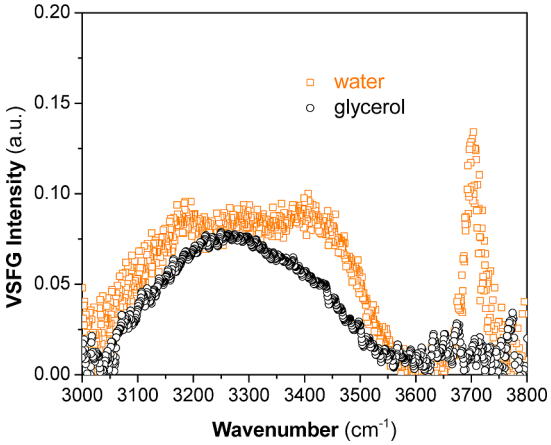

Figure 1. VSFG spectra of the neat air/water and air/glycerol interfaces in the OH stretching region (3000−3800 cm^{-1}). Glycerol spectrum was smoothed using a 15 data points Savitzky−Golay filtering.

Additionally, by comparing with the neat water VSFG spectrum, one can notice in the glycerol spectrum the absence of the sharp peak located at 3700 cm^{-1}. This is a key spectral feature in the neat water VSFG spectrum that has been assigned to dangling OH groups that protrude out into the vapor phase and comprise ~25% of the topmost surface water molecules.[51,52] The lack of a similar spectral feature in the glycerol spectrum indicates the absence of dangling OH groups, although this does not preclude other considerations such as a possible isotropic orientation or parallel (anisotropic) orientation of these groups in the surface plane. Both of these scenarios are difficult to rule out due to low signal-to-noise ratios of complementary VSFG polarization studies.[14] A molecular dynamics study of the glycerol surface revealed that it is more likely to find CH and CH_2 groups than the glycerol oxygens (OH groups) at the neat glycerol surface.[53] This is consistent with the small VSFG signal intensity found in the high frequency region of the VSFG spectrum. Moreover, on the basis of the findings from VSFG spectra of glycerol and other alcohols, Baldelli et al.[13,14] and Stanners et al. (for studies of methanol and ethanol)[54] also suggested that very few dangling OH bonds should be exposed at the neat glycerol surface.

Although the apparent spectral shape and bandwidth of the glycerol VSFG spectrum in the OH stretching region is obviously different from that of water, it still suggests that there are strong and weak hydrogen bonds as one moves from the low to the high frequency region. The narrower band of glycerol relative to water is indicative of narrower distribution of hydrogen bonding strengths. Additionally, the overall intensity of the glycerol spectrum is slightly lower than that of water, suggesting a lower OH density relative to neat water, as is expected due to the replacement of water by glycerol. Yet, variation from interference effects inherent with VSFG spectroscopy,[36,37,55−57] oscillator strength, and reduced signal from increased scattering due to glycerol aggregation states should also be considered.[8,10,58] A similar intensity reduction was also observed in a previous study of water and ethanol using VSFG spectroscopy.[59]

3.2. Salty Glycerol and Water Solutions. To understand the effect of halide anion on glycerol interfacial solvation, VSFG spectra of two salty glycerol solutions (NaBr and NaI) at two different concentrations (1 and 2 M) were studied (Figure 2a), together with the spectrum of pure glycerol as reference. The VSFG spectra of the salty glycerol solutions have a similar asymmetric spectral shape as that of pure glycerol with a larger signal enhancement in the lower frequency region, but differ significantly in their overall signal intensity. Note that for the glycerol solutions, the 2 M NaBr is similar in intensity to the 1 M NaI, but in general, there is an increase in intensity with concentration given the same salt.

A comparison between the 1 M NaBr and NaI glycerol VSFG spectra shows a similar intensity increase in the low frequency region centered at 3250 cm^{-1} for both anions, while the higher frequency region above 3400 cm^{-1} experiences a slightly larger intensity increase in the case of I^- ions (Figure 2a). The enhancement in the higher frequency region thus appears to be strongly ion- and concentration-dependent. These intensity observations suggest a correlation to halide anion size and polarizability where increasing size and polarizability give rise to increasing intensity. This is reminiscent of previously published results from aqueous halide surfaces.[26] The relatively large noise at 3600−3800 cm^{-1} in the VSFG spectra of glycerol solutions is due to the lower energy at the high frequency side of the IR laser pulses used in the experiments. Particularly, the noise associated with

dx.doi.org/10.1021/jp4020228 | J. Phys. Chem. A 2013, 117, 6346−6353

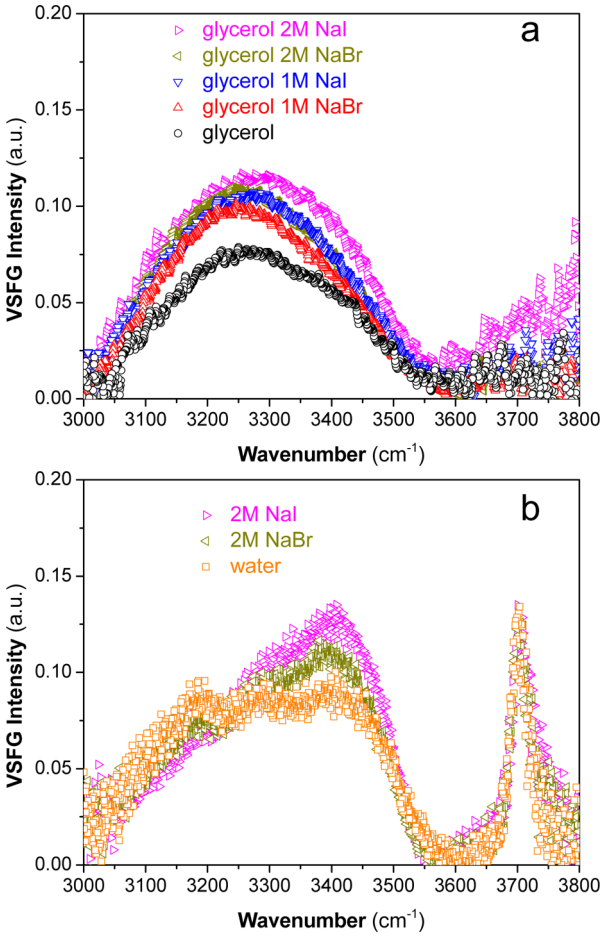

Figure 2. (a) VSFG spectra of sodium halide glycerol solutions in the OH stretching region (smoothed using a 15 data points Savitzky–Golay filtering). (b) VSFG spectra of sodium halide aqueous solutions in the OH stretching region. The VSFG spectra of neat glycerol and water are also shown as reference.

the 2 M NaI is higher than others and likely arises from light scattering of the concentrated solution.

For comparison to the aqueous salt solutions, the VSFG spectra of the OH stretching region of 2 M aqueous NaBr and NaI in the OH stretching are shown in Figure 2b, with the neat water spectrum shown for reference. As with the salty glycerol spectra (Figure 2a), an enhancement of the intensity is also observed in these spectra, but solely in the higher frequency region. However, the 2 M NaI solution VSFG spectrum is enhanced more than the 2 M NaBr solution. This observation is consistent with previously published work.[26,28] The dangling OH intensity remains generally unchanged for aqueous NaBr and NaI.

The signal enhancement in VSFG spectra observed for both salty glycerol and aqueous solutions reveals that the OH stretching band is highly sensitive to the incorporation of the halide anions within their interfaces. These spectra also indicate that the enhancement varies with the halide anion identity and that increasing the concentration also increases the enhancement for each sodium halide measured, thus revealing similarities in solvation characteristics between glycerol and water. However, the halide salts increase the intensity in the lower frequency region of the salty glycerol spectra, but a decrease is seen in the corresponding salty aqueous spectra. This might suggest that the halide salts reorganize differently the hydrogen bonding network of glycerol than for water. This is discussed further below. However, this assertion would clearly need further experimental and computational verifications beyond the scope of the current study; phase-sensitive VSFG (PS-VSFG) spectroscopy studies are underway in our laboratory to test this.

Yet, in order to further explore the origins of this VSFG signal enhancement, comparison of the VSFG spectral signature with that from bulk Raman and IR spectroscopic measurements is helpful. This comparison is justified by the fact that the (orientationally averaged) molecular hyperpolarizability (β_{ijk}), which is proportional to the VSFG intensity, is related to the product of Raman polarizability (α_{ij}) and IR dipole (μ_k) transition moment strength of interfacial molecules:[55]

$$\beta_{ijk} = \langle g|\alpha_{ij}|\nu\rangle\langle\nu|\mu_k|g\rangle \quad (1)$$

where ν and g are the excited and ground vibrational states, respectively. This gives rise to the VSFG selection rule according to which any vibrational mode of an interfacial species must be both Raman and IR active in order to be VSFG allowed. Therefore, Raman and IR spectroscopic evaluation of the salty glycerol solutions provide knowledge of the bulk solvation environment and also provide a basis for comparison for the interfacial presence of the ions because of the theoretical relationship between Raman and IR with VSFG.

The Raman and Raman difference spectra of pure glycerol and 1 and 2 M sodium halide glycerol solutions were measured and are shown in Figure 3. The pure glycerol exhibits a broad OH stretching band consisting of two main peaks at ~3260 and ~3460 cm^{-1}. On the basis of polarization Raman studies, Mendelovici et al. analyzed this broad band and decomposed it into two subpeaks at 3240 and 3407 cm^{-1}, which were assigned to symmetric and antisymmetric OH stretches, respectively.[11] In contrast, Kojima[10] and Mudalige and Pemberton[60] fit the Raman spectrum in this region to three subpeaks centered, respectively, at 3230, 3340, and 3440 cm^{-1}. The former two were assigned to the OH vibrations of oligomers with an aggregation number greater than two, while the latter one was associated to the modes of dimeric units.[10,60] Here, similarly to the assignment of water Raman spectra, a more general assignment of the OH stretching of glycerol is made where lower and higher spectral frequency regions are thought to be representative, respectively, of strongly and weakly hydrogen-bonded solvent networks.

With respect to the salty glycerol solutions shown in Figure 3a, an increase in Raman intensity is associated with anion identity (size and polarizability) and concentration, which is consistent with previously published Raman data of halide ions in methanol.[61] In addition, the Raman spectral changes induced by the solvated salts, namely, an increase in intensity with halide type and concentration, appear similar to those observed for the aqueous halide solution spectra,[26] as shown in Figure 3c. This similarity is also emphasized by the salty water difference spectra shown in Figure 3d. Finally, one can note the small blue and red shifts of the 3200 and 3450 cm^{-1} peaks, respectively, for the salty glycerol spectra, although difficult to discern due to the broad character of the glycerol higher frequency region and the intensity decrease of the lower frequency band.

On the basis of the comparison between salty glycerol and aqueous solutions Raman spectra, the significant increase at ~3450 cm^{-1} is highly suggestive of an increase in the OH

dx.doi.org/10.1021/jp4020228 | J. Phys. Chem. A 2013, 117, 6346–6353

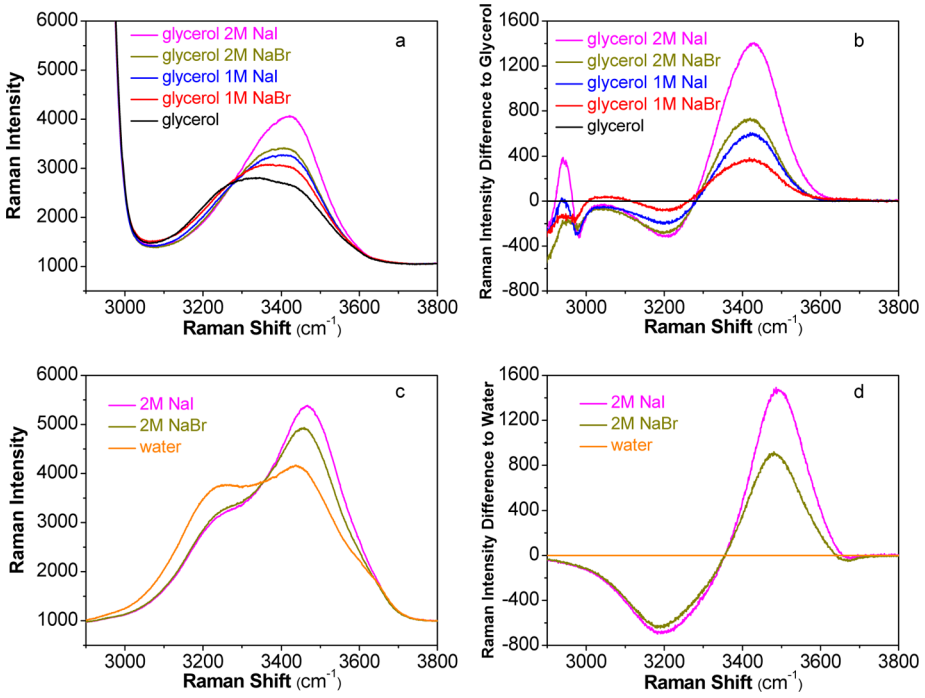

Figure 3. (a) Raman spectra of sodium halide glycerol solutions. (b) Raman difference spectra of sodium halide glycerol solutions relative to pure glycerol. (c) Raman spectra of sodium halide aqueous solutions. (d) Raman difference spectra of sodium halide aqueous solutions relative to pure water.

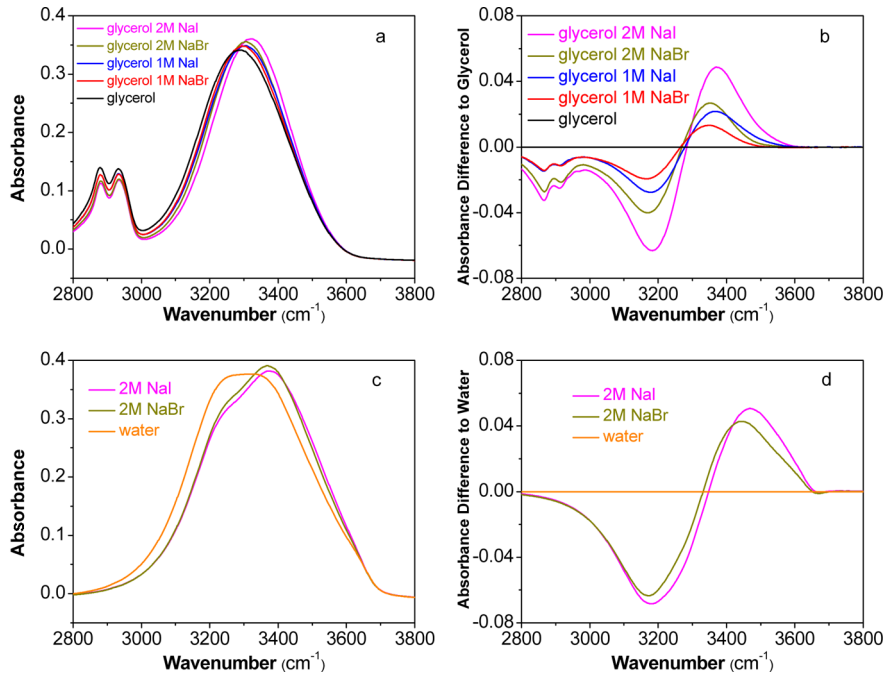

Figure 4. (a) FTIR spectra of sodium halide glycerol solutions. (b) FTIR difference spectra of sodium halide glycerol solutions relative to pure glycerol. (c) FTIR spectra of sodium halide aqueous solutions. (d) FTIR difference spectra of sodium halide aqueous solutions relative to pure water.

Raman transition moment strength. Recall that the 3400 cm^{-1} region is correlated with an increase in anion size and polarizability,[26] for both solvents. For salty water solutions, this observation has been explored in the literature experimentally[26,62] and theoretically.[62] Thus, the Raman spectral differences of Figure 3 are attributed to differences between the solvation of halide anions in glycerol versus that of water, although both solvents are thought to prefer monodentate binding.[16,63] Using MD simulations and Raman spectroscopy of halide aqueous solutions, Smith et al. proposed that the electric field effects on the first solvation shell result in the most significant changes in Raman spectra due to dissolved salts.[62] Thus, one might conclude that both the similarities and the differences between the Raman spectra shown here of salty glycerol and aqueous solutions results from the character of the hydrogen bonding in the first solvation shells of glycerol and

dx.doi.org/10.1021/jp4020228 | J. Phys. Chem. A 2013, 117, 6346−6353

water solutions. Given that larger differences are observed in the aqueous solution Raman spectra when comparing Figure 3b and d, it is suggested that water molecules are slightly more perturbed by the addition of halide salts relative to glycerol in the bulk environment (see Figure 3d, 3200 cm^{-1} region). In other words, water is more easily reorganized by the ions, as might be expected due to the fact that glycerol−glycerol interactions involve additional van der Waals forces (as these become larger as the mass and size increase), and per molecule, glycerol has additional sites for hydrogen bonding. Yet, both solvents appear to be impacted primarily in the higher frequency region, suggesting somewhat similar solvation properties. The enhanced intensity change in more concentrated salty glycerol solutions (as well as in water) can be readily understood due to the increased number of ions interacting with solvent molecules.

The IR spectra of salty glycerol and aqueous solutions as well as their IR difference spectra are shown in Figure 4. The spectra of glycerol and its salty solutions show a very broad band around 3300 cm^{-1} (Figure 4a). Less intensity enhancement is observed here relative to the Raman spectra although the bands are blue-shifted relative to pure glycerol and pure water (Figure 4a,c). From the IR difference spectra in Figure 4b,d, the intensity changes at ∼3200 and ∼3400 cm^{-1} are somewhat comparable in both glycerol and water, although slightly more for water in the low frequency region. The overall observed spectral differences in the Raman and IR spectra are generally attributed to their selection rules, polarizability change versus change in dipole moment during the vibration; however, just as observed in the Raman spectra for both solvents, water appears to be perturbed to a greater extent as evidenced by the slightly larger change in the IR spectra.

Comparison of the Raman and IR spectra to the VSFG data reveals that the VSFG spectral changes upon addition of the salts reflect in some ways the changes observed in the Raman and IR data. However, the VSFG intensity enhancement in the 3200 cm^{-1} region is not necessarily predicted from an analysis of the bulk spectroscopic data. In the interfacial region, the glycerol molecules may be oriented in an electric field as is now being suggested for other aqueous interfaces.[36,64−66] A study on $CaCl_2$ and NaCl aqueous solutions combining conventional and phase-sensitive VSFG (PS-VSFG) spectroscopy study by Hua et al. might provide some insights.[65] PS-VSFG spectroscopy provides orientational information about the net OH transition moment from which ion distributions within the interfacial region can be inferred. In Hua et al.'s work,[65] an enhancement of the OH stretch region in the PS-VSFG Im $\chi^{(2)}$ spectra was observed in the spectra of $CaCl_2$ and NaCl aqueous solutions compared to pure water and revealed that a greater alignment of interfacial water molecules was due to the presence of an interfacial electric field induced by the ion's spatial distribution. This interpretation is also supported by Tian et al.'s study on atmospherically relevant ions in salt solutions.[66] It can be argued here that halide salts possess similar effects at the air/glycerol interface and that sodium and halide ion distributions create an electric field in the interfacial region that helps to align the glycerol OH groups (unpublished preliminary PS-VSFG data are suggestive of this). Since VSFG spectroscopy is interface specific and responsive to an environment lacking centrosymmetry such as an interface, the more ordered OH groups of interfacial glycerol molecules due to the electric field created by the separation of cations and anions could give rise to a higher intensity in VSFG spectra. This is supported indirectly by Cwiklik et al.[67] who investigated the surface of NaI solution of ethylene glycol using MD simulations. The density profiles showed that I^- ions mainly populated the interfacial region with their counter cations Na^+ located ∼8 Å below them. This separation could create an interfacial region where the transition dipole moments of ethylene glycol OH groups, and similarly glycerol OH groups, become more aligned as well. As stated above, PS-VSFG data needs to confirm this speculation, as the real part of the refractive index can obscure interpretation from conventional VSFG data.[65]

3.2.1. Surface Tension of Salty Glycerol and Aqueous Solutions. Considering that surface tension is a thermodynamic macroscopic indicator of the surface prevalence for a given solute, it could provide complementary information for the above-discussed molecular-level spectroscopic results regarding sodium halides. The surface tension measurements of NaBr and NaI glycerol and aqueous solutions relative to the pure solvents are shown in Figure 5. For the salty glycerol and aqueous solutions, an increase in the surface tension with increasing concentration is observed. However, the surface tension of salty glycerol solutions does not increase to the same extent as that from aqueous solutions. This is not necessarily surprising because glycerol is expected to be surface active. Halide surface accumulation followed by a depletion region in the interface is consistent with theoretical work by Jungwirth and Tobias.[24,25] The increase relative to pure water in the presence of sodium halides is obviously higher than that relative to pure glycerol. However, the trend that I^- ions produce a less significant surface tension increase compared to Br^- ions holds for both glycerol and water, suggesting that I^- ions segregates more than Br^- ions to the surface.[24,25,68]

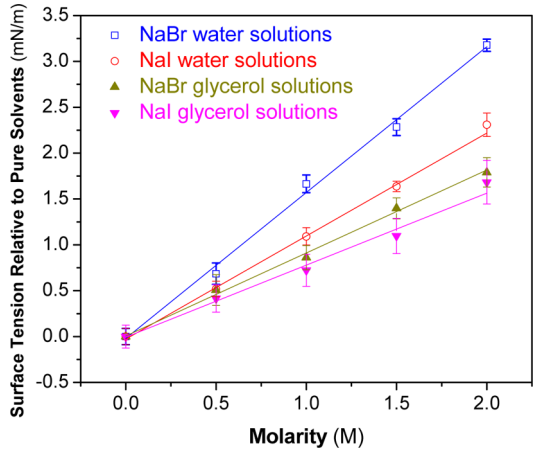

Figure 5. Surface tensions of sodium halide glycerol and aqueous solutions relative to their respective pure solvents.

CONCLUSIONS

Here, bromide and iodide anions are shown to exist at the air/glycerol interface and to perturb the glycerol hydrogen bonding network. The more polarizable halide I^- has a larger impact on the VSFG spectrum in the OH stretch region relative to Br^-, suggesting a larger surface propensity of I^- than Br^- in the air/glycerol interfacial region. However, the difference observed at ∼3200 cm^{-1} between the air/glycerol and the air/water VSFG spectra indicates a different distribution of hydrogen bonding strengths in the interfacial region. Additionally, surface tension

dx.doi.org/10.1021/jp4020228 | J. Phys. Chem. A 2013, 117, 6346−6353

measurements suggest a similar trend in surface excess of halide anions for the air/glycerol and air/water interfaces. Moreover, the VSFG results reveal that glycerol and water share similar trends in terms of hydrogen bonding disruption, but their impact on water organization in the interfacial region in the presence of halide anions is slightly different. Additional experiments (phase sensitive VSFG and possibly high pressure X-ray photoelectron spectroscopy) in addition to theoretical work would be advantageous to further investigate the relative propensity of halide anions at the air/glycerol interface.

AUTHOR INFORMATION

Corresponding Author

*(H.C.A.) E-mail: allen@chemistry.ohio-state.edu.

Notes

The authors declare no competing financial interest.

ACKNOWLEDGMENTS

We thank the National Science Foundation, Division of Chemistry, Environmental Chemical Sciences (ECS) program (grant CHE-1111762) for funding this research.

REFERENCES

(1) Miner, C. S.; Dalton, N. N. *Glycerol*; Reinhold Pub. Corp.: New York, 1953.

(2) *Physical Properties of Glycerine and Its Solutions*; Glycerine Producers' Association: New York, 1963.

(3) Silva, M. d. S.; Ferreira, P. C. *Glycerol: Production, Structure, and Applications*; Nova Science Publishers: New York, 2012.

(4) Vargaftik, N. B.; Volkov, B. N.; Voljak, L. D. International Tables of the Surface-Tension of Water. *J. Phys. Chem. Ref. Data* **1983**, *12*, 817−820.

(5) Archer, D. G.; Wang, P. The Dielectric Constant of Water and Debye-Huckel Limiting Law Slopes. *J. Phys. Chem. Ref. Data* **1990**, *19*, 371−411.

(6) Champeney, D. C.; Joarder, R. N.; Dore, J. C. Structural Studies of Liquid D-Glycerol by Neutron Diffraction. *Mol. Phys.* **1986**, *58*, 337−347.

(7) Root, L. J.; Stillinger, F. H. Short-Range Order in Glycerol: a Molecular-Dynamics Study. *J. Chem. Phys.* **1989**, *90*, 1200−1208.

(8) Chelli, R.; Procacci, P.; Cardini, G.; Califano, S. Glycerol Condensed Phases Part II. A Molecular Dynamics Study of the Conformational Structure and Hydrogen Bonding. *Phys. Chem. Chem. Phys.* **1999**, *1*, 879−885.

(9) Soltwisch, M.; Steffen, B. The X-Ray Structure Factor of Liquid Glycerol. *Z. Naturforsch., A: Phys. Sci.* **1981**, *36*, 1045−1051.

(10) Kojima, S. Anomalous Behavior of the O−H Stretching Vibrational-Mode in the Liquid-Glass Transition of Glycerol. *J. Mol. Struct.* **1993**, *294*, 193−195.

(11) Mendelovici, E.; Frost, R. L.; Kloprogge, T. Cryogenic Raman Spectroscopy of Glycerol. *J. Raman Spectrosc.* **2000**, *31*, 1121−1126.

(12) Kataoka, Y.; Kitadai, N.; Hisatomi, O.; Nakashima, S. Nature of Hydrogen Bonding of Water Molecules in Aqueous Solutions of Glycerol by Attenuated Total Reflection (ATR) Infrared Spectroscopy. *Appl. Spectrosc.* **2011**, *65*, 436−441.

(13) Baldelli, S.; Schnitzer, C.; Shultz, M. J.; Campbell, D. J. Sum Frequency Generation Investigation of Glycerol/Water Surfaces. *J. Phys. Chem. B* **1997**, *101*, 4607−4612.

(14) Oh-e, M.; Yokoyama, H.; Baldelli, S. Structure of the Glycerol Liquid/Vapor Interface Studied by Sum-Frequency Vibrational Spectroscopy. *Appl. Phys. Lett.* **2004**, *84*, 4965−4967.

(15) Krebs, T.; Andersson, G.; Morgner, H. Electron Energy Loss Spectroscopy of Liquid Glycerol. *Chem. Phys.* **2007**, *340*, 181−186.

(16) Okan, S. E.; Salmon, P. S. A Neutron-Diffraction Study on the Structure of Cl^- Solutions in Hydrogen-Bonded Molecular-Solvents. *J. Phys.: Condens. Matter* **1994**, *6*, 3839−3848.

(17) Okan, S. E.; Salmon, P. S.; Champeney, D. C.; Petri, I. The Solvation of Cations in Hydrogen-Bonded Molecular-Solvents: a Neutron-Diffraction Study on the Structure of Ni^{2+} Solutions in Ethylene-Glycol and in Glycerol. *Mol. Phys.* **1995**, *84*, 325−343.

(18) Dempsey, L. P.; Brastad, S. M.; Nathanson, G. M. Interfacial Acid Dissociation and Proton Exchange Following Collisions of DCl with Salty Glycerol and Salty Water. *J. Phys. Chem. Lett.* **2011**, *2*, 622−627.

(19) Muenter, A. H.; DeZwaan, J. L.; Nathanson, G. M. Interfacial Interactions of DCl with Salty Glycerol Solutions of KI, NaI, LiI, and NaBr. *J. Phys. Chem. C* **2007**, *111*, 15043−15052.

(20) Muenter, A. H.; DeZwaan, J. L.; Nathanson, G. M. Collisions of DCl with Pure and Salty Glycerol: Enhancement of Interfacial D → H Exchange by Dissolved NaI. *J. Phys. Chem. B* **2006**, *110*, 4881−4891.

(21) Brastad, S. M.; Albert, D. R.; Huang, M. W.; Nathanson, G. M. Collisions of DCl with a Solution Covered with Hydrophobic and Hydrophilic Ions: Tetrahexylammonium Bromide in Glycerol. *J. Phys. Chem. A* **2009**, *113*, 7422−7430.

(22) Nathanson, G. M.; Davidovits, P.; Worsnop, D. R.; Kolb, C. E. Dynamics and Kinetics at the Gas−Liquid Interface. *J. Phys. Chem.* **1996**, *100*, 13007−13020.

(23) Dempsey, L. P.; Faust, J. A.; Nathanson, G. M. Near-Interfacial Halogen Atom Exchange in Collisions of Cl_2 with 2.7 M NaBr-Glycerol. *J. Phys. Chem. B* **2012**, *116*, 12306−12318.

(24) Jungwirth, P.; Tobias, D. J. Molecular Structure of Salt Solutions: A New View of the Interface with Implications for Heterogeneous Atmospheric Chemistry. *J. Phys. Chem. B* **2001**, *105*, 10468−10472.

(25) Jungwirth, P.; Tobias, D. J. Ions at the Air/Water Interface. *J. Phys. Chem. B* **2002**, *106*, 6361−6373.

(26) Liu, D. F.; Ma, G.; Levering, L. M.; Allen, H. C. Vibrational Spectroscopy of Aqueous Sodium Halide Solutions and Air−Liquid Interfaces: Observation of Increased Interfacial Depth. *J. Phys. Chem. B* **2004**, *108*, 2252−2260.

(27) Schnitzer, C.; Baldelli, S.; Shultz, M. J. Sum Frequency Generation of Water on NaCl, $NaNO_3$, $KHSO_4$, HCl, HNO_3, and H_2SO_4 Aqueous Solutions. *J. Phys. Chem. B* **2000**, *104*, 585−590.

(28) Raymond, E. A.; Richmond, G. L. Probing the Molecular Structure and Bonding of the Surface of Aqueous Salt Solutions. *J. Phys. Chem. B* **2004**, *108*, 5051−5059.

(29) Tian, C. S.; Ji, N.; Waychunas, G. A.; Shen, Y. R. Interfacial Structures of Acidic and Basic Aqueous Solutions. *J. Am. Chem. Soc.* **2008**, *130*, 13033−13039.

(30) Bian, H. T.; Feng, R. R.; Xu, Y. Y.; Guo, Y.; Wang, H. F. Increased Interfacial Thickness of the NaF, NaCl and NaBr Salt Aqueous Solutions Probed with Non-Resonant Surface Second Harmonic Generation (SHG). *Phys. Chem. Chem. Phys.* **2008**, *10*, 4920−4931.

(31) Allen, H. C.; Casillas-Ituarte, N. N.; Sierra-Hernandez, M. R.; Chen, X. K.; Tang, C. Y. Shedding Light on Water Structure at Air−Aqueous Interfaces: Ions, Lipids, and Hydration. *Phys. Chem. Chem. Phys.* **2009**, *11*, 5538−5549.

(32) Hommel, E. L.; Ma, G.; Allen, H. C. Broadband Vibrational Sum Frequency Generation Spectroscopy of a Liquid Surface. *Anal. Sci.* **2001**, *17*, 1325−1329.

(33) Ma, G.; Allen, H. C. Surface Studies of Aqueous Methanol Solutions by Vibrational Broad Bandwidth Sum Frequency Generation Spectroscopy. *J. Phys. Chem. B* **2003**, *107*, 6343−6349.

(34) Tang, C. Y.; Allen, H. C. Ionic Binding of Na^+ Versus K^+ to the Carboxylic Acid Headgroup of Palmitic Acid Monolayers Studied by Vibrational Sum Frequency Generation Spectroscopy. *J. Phys. Chem. A* **2009**, *113*, 7383−7393.

(35) Adamson, A. W.; Gast, A. P. *Physical Chemistry of Surfaces*; Wiley: New York, 1997.

(36) Ji, N.; Ostroverkhov, V.; Tian, C. S.; Shen, Y. R. Characterization of Vibrational Resonances of Water-Vapor Interfaces by Phase-Sensitive Sum-Frequency Spectroscopy. *Phys. Rev. Lett.* **2008**, *100*, 096102.

(37) Shen, Y. R.; Ostroverkhov, V. Sum-Frequency Vibrational Spectroscopy on Water Interfaces: Polar Orientation of Water Molecules at Interfaces. *Chem. Rev.* **2006**, *106*, 1140−1154.
(38) Watry, M. R.; Tarbuck, T. L.; Richmond, G. I. Vibrational Sum-Frequency Studies of a Series of Phospholipid Monolayers and the Associated Water Structure at the Vapor/Water Interface. *J. Phys. Chem. B* **2003**, *107*, 512−518.
(39) Sovago, M.; Campen, R. K.; Bakker, H. J.; Bonn, M. Hydrogen Bonding Strength of Interfacial Water Determined with Surface Sum-Frequency Generation. *Chem. Phys. Lett.* **2009**, *470*, 7−12.
(40) Tang, C. Y.; Huang, Z. S.; Allen, H. C. Interfacial Water Structure and Effects of Mg^{2+} and Ca^{2+} Binding to the COOH Headgroup of a Palmitic Acid Monolayer Studied by Sum Frequency Spectroscopy. *J. Phys. Chem. B* **2011**, *115*, 34−40.
(41) Chen, X. K.; Hua, W.; Huang, Z. S.; Allen, H. C. Interfacial Water Structure Associated with Phospholipid Membranes Studied by Phase-Sensitive Vibrational Sum Frequency Generation Spectroscopy. *J. Am. Chem. Soc.* **2010**, *132*, 11336−11342.
(42) Pieniazek, P. A.; Tainter, C. J.; Skinner, J. L. Surface of Liquid Water: Three-Body Interactions and Vibrational Sum-Frequency Spectroscopy. *J. Am. Chem. Soc.* **2011**, *133*, 10360−10363.
(43) Casillas-Ituarte, N. N.; Callahan, K. M.; Tang, C. Y.; Chen, X. K.; Roeselova, M.; Tobias, D. J.; Allen, H. C. Surface Organization of Aqueous $MgCl_2$ and Application to Atmospheric Marine Aerosol Chemistry. *Proc. Natl. Acad. Sci. U.S.A.* **2010**, *107*, 6616−6621.
(44) Ishiyama, T.; Morita, A. Molecular Dynamics Study of Gas-Liquid Aqueous Sodium Halide Interfaces. II. Analysis of Vibrational Sum Frequency Generation Spectra. *J. Phys. Chem. C* **2007**, *111*, 738−748.
(45) Ishiyama, T.; Morita, A. Analysis of Anisotropic Local Field in Sum Frequency Generation Spectroscopy with the Charge Response Kernel Water Model. *J. Chem. Phys.* **2009**, *131*, 244714.
(46) Ishiyama, T.; Morita, A. Vibrational Spectroscopic Response of Intermolecular Orientational Correlation at the Water Surface. *J. Phys. Chem. C* **2009**, *113*, 16299−16302.
(47) Tian, C. S.; Shen, Y. R. Sum-Frequency Vibrational Spectroscopic Studies of Water/Vapor Interfaces. *Chem. Phys. Lett.* **2009**, *470*, 1−6.
(48) Sovago, M.; Campen, R. K.; Wurpel, G. W. H.; Mueller, M.; Bakker, H. J.; Bonn, M. Comment on "Vibrational Response of Hydrogen-Bonded Interfacial Water Is Dominated by Intramolecular Coupling"- Reply. *Phys. Rev. Lett.* **2008**, *101*, 139401.
(49) Sovago, M.; Campen, R. K.; Wurpel, G. W. H.; Muller, M.; Bakker, H. J.; Bonn, M. Vibrational Response of Hydrogen-Bonded Interfacial Water Is Dominated by Intramolecular Coupling. *Phys. Rev. Lett.* **2008**, *100*, 173901.
(50) Verreault, D.; Hua, W.; Allen, H. C. From Conventional to Phase-Sensitive Vibrational Sum Frequency Generation Spectroscopy: Probing Water Organization at Aqueous Interfaces. *J. Phys. Chem. Lett.* **2012**, *3*, 3012−3028.
(51) Wei, X.; Miranda, P. B.; Zhang, C.; Shen, Y. R. Sum-Frequency Spectroscopic Studies of Ice Interfaces. *Phys. Rev. B* **2002**, *66*, 085401.
(52) Du, Q.; Freysz, E.; Shen, Y. R. Surface Vibrational Spectroscopic Studies of Hydrogen-Bonding and Hydrophobicity. *Science* **1994**, *264*, 826−828.
(53) Benjamin, I.; Wilson, M.; Pohorille, A. Scattering of Ne from the Liquid: Vapor Interface of Glycerol: A Molecular Dynamics Study. *J. Chem. Phys.* **1994**, *100*, 6500−6507.
(54) Stanners, C. D.; Du, Q.; Chin, R. P.; Cremer, P.; Somorjai, G. A.; Shen, Y. R. Polar Ordering at the Liquid-Vapor Interface of *N*-Alcohols (C-1-C-8). *Chem. Phys. Lett.* **1995**, *232*, 407−413.
(55) Shen, Y. R. *The Principles of Nonlinear Optics*; J. Wiley: New York, 1984.
(56) Shen, Y. R. Surface-Properties Probed by 2nd-Harmonic and Sum-Frequency Generation. *Nature* **1989**, *337*, 519−525.
(57) Nihonyanagi, S.; Yamaguchi, S.; Tahara, T. Direct Evidence for Orientational Flip-Flop of Water Molecules at Charged Interfaces: A Heterodyne-Detected Vibrational Sum Frequency Generation Study. *J. Chem. Phys.* **2009**, *130*, 204704/1−204704/5.
(58) Uchino, T.; Yoko, T. Low-Frequency Raman Scattering and the Fast Relaxation Process in Glycerol. *Science* **1996**, *273*, 480−483.
(59) Ju, S. S.; Wu, T. D.; Yeh, Y. L.; Wei, T. H.; Huang, J. Y.; Lin, S. H. Sum Frequency Vibrational Spectroscopy of the Liquid-Air Interface of Aqueous Solutions of Ethanol in the Oh Region. *J. Chin. Chem. Soc.* **2001**, *48*, 625−629.
(60) Mudalige, A.; Pemberton, J. E. Raman Spectroscopy of Glycerol/D_2O Solutions. *Vib. Spectrosc.* **2007**, *45*, 27−35.
(61) Hidaka, F.; Yoshimura, Y.; Kanno, H. Anionic Effects on Raman Od Stretching Spectra for Alcoholic Lix Solutions (X = Cl^-, Br^-, I^-, ClO_4^-, NO_3^-, and CH_3COO^-). *J. Solution Chem.* **2003**, *32*, 239−251.
(62) Smith, J. D.; Saykally, R. J.; Geissler, P. L. The Effects of Dissolved Halide Anions on Hydrogen Bonding in Liquid Water. *J. Am. Chem. Soc.* **2007**, *129*, 13847−13856.
(63) Sharpe, A. G. The Solvation of Halide-Ions and Its Chemical Significance. *J. Chem. Educ.* **1990**, *67*, 309−315.
(64) Hua, W.; Chen, X. K.; Allen, H. C. Phase-Sensitive Sum Frequency Revealing Accommodation of Bicarbonate Ions, and Charge Separation of Sodium and Carbonate Ions within the Air/Water Interface. *J. Phys. Chem. A* **2011**, *115*, 6233−6238.
(65) Hua, W.; Jubb, A. M.; Allen, H. C. Electric Field Reversal of Na_2SO_4, $(NH_4)_2SO_4$, and Na_2CO_3 Relative to $CaCl_2$ and NaCl at the Air/Aqueous Interface Revealed by Heterodyne Detected Phase-Sensitive Sum Frequency. *J. Phys. Chem. Lett.* **2011**, *2*, 2515−2520.
(66) Tian, C. S.; Byrnes, S. J.; Han, H. L.; Shen, Y. R. Surface Propensities of Atmospherically Relevant Ions in Salt Solutions Revealed by Phase-Sensitive Sum Frequency Vibrational Spectroscopy. *J. Phys. Chem. Lett.* **2011**, *2*, 1946−1949.
(67) Cwiklik, L.; Andersson, G.; Dang, L. X.; Jungwirth, P. Segregation of Inorganic Ions at Surfaces of Polar Nonaqueous Liquids. *ChemPhysChem* **2007**, *8*, 1457−1463.
(68) Pegram, L. M.; Record, M. T. Partitioning of Atmospherically Relevant Ions between Bulk Water and the Water/Vapor Interface. *Proc. Natl. Acad. Sci. U.S.A.* **2006**, *103*, 14278−14281.